Cancer Research

Cancer-Associated Fibroblasts Expressing CXCL14 Rely upon NOS1-Derived Nitric Oxide Signaling for Their Tumor-Supporting Properties

Martin Augsten[1], Elin Sjöberg[1], Oliver Frings[1], Sabine U. Vorrink[1], Jeroen Frijhoff[1], Eleonor Olsson[2], Åke Borg[2], and Arne Östman[1]

Abstract

Cancer-associated fibroblasts (CAF) stimulate tumor growth and metastasis. Signals supporting CAF function are thus emerging as candidate therapeutic targets in the tumor microenvironment. The chemokine CXCL14 is a potent inducer of CAF protumorigenic functions. This study is aimed at learning how the protumoral functions of CXCL14-expressing CAF are maintained. We found that the nitric oxide synthase NOS1 is upregulated in CXCL14-expressing CAF and in fibroblasts stimulated with CXCL14. Induction of Nos1 was associated with oxidative stress and occurred together with activation of NRF2 and HIF1α signaling in CXCL14-expressing CAF. Genetic or pharmacologic inhibition of NOS1 reduced the growth of CXCL14-expressing fibroblasts along with their ability to promote tumor formation following coinjection with prostate or breast cancer cells. Tumor analysis revealed reduced macrophage infiltration, with NOS1 downregulation in CXCL14-expressing CAF and lymphangiogenesis as a novel component of CXCL14-promoted tumor growth. Collectively, our findings defined key components of a signaling network that maintains the protumoral functions of CXCL14-stimulated CAF, and they identified NOS1 as intervention target for CAF-directed cancer therapy. *Cancer Res; 74(11); 2999–3010. ©2014 AACR.*

Introduction

CXCL14, also designated BRAK, MIP-2γ, or BMAC, is an orphan member of the CXC chemokine subfamily. Earlier studies have indicated a broad chemotactic activity for various cell types, including immature dendritic cells, monocytes, macrophages, and natural killer cells, but not T cells (1). However, analyses of *CXCL14* knockout mice have indicated that CXCL14 is not required for dendritic cell and macrophage function under *in vivo* inflammatory conditions (2). The functional roles of CXCL14 in tumor biology have been addressed in a number of studies and indicate context-dependent pro- or antitumoral effects (1). Some studies, analyzing effects of CXCL14 overexpression in cancer cells, have reported antitumoral and antiangiogenic effects (3–6). Protumoral effects of CXCL14 have been suggested based on evidence for upregulation of CXCL14 in the tumor stroma and cancer-associated fibroblasts (CAF; refs. 7, 8). Experimental support for this notion was obtained in our previous study, which demonstrated enhanced protumoral effects of CXCL14-producing fibroblasts in a prostate cancer animal model (8). Tumors composed of LNCaP prostate cancer cells and fibroblasts overexpressing CXCL14 (LNCaP/NIH-CXCL14) developed much faster than control tumors (LNCaP/NIH-ctr) and displayed enhanced ingrowth of vessels and monocytes. Further analyses confirmed increased activity of CXCL14 fibroblasts, as compared with control fibroblasts, with regard to chemoattraction of monocytes and stimulation of angiogenesis (8). The intracellular signaling that mediates the effects of CXCL14 is poorly characterized, so far pointing only to CXCL14-induced calcium influx and activation of NF-κB and extracellular signal–regulated kinase (ERK; refs. 8, 9). The aim of this study was to further characterize the mechanisms involved in the protumoral effects of fibroblast-derived CXCL14. We compared the effects of control (NIH-ctr) fibroblasts and CXCL14-expressing fibroblasts (NIH-CXCL14) in tissue culture and animal xenograft models, and identified NOS1 as a novel component of the intracellular signaling that contributes to the tumor-promoting effects of CXCL14-expressing fibroblasts.

Materials and Methods

Cell lines and chemicals

NIH-ctr and NIH-CXCL14 fibroblasts were established as previously described (8). The NIH-ctr, NIH-CXCL14, and derivatives thereof were propagated in Dulbecco's Modified Eagle

Authors' Affiliations: [1]Department of Oncology-Pathology, Karolinska Institutet, Stockholm; [2]Department of Oncology, Lund University, Lund, Sweden

Note: Supplementary data for this article are available at Cancer Research Online (http://cancerres.aacrjournals.org/).

Current address for Sabine U. Vorrink: Interdisciplinary Graduate Program in Human Toxicology, The University of Iowa, Iowa City, Iowa

Corresponding Author: Martin Augsten, Karolinska Institutet, Cancer Center Karolinska, Karolinska Universitetsjukhuset, 17176 Stockholm, Sweden. Phone: 46-8-517-70-246; Fax: 46-8-33-90-31; E-mail: Martin.Augsten@ki.se

doi: 10.1158/0008-5472.CAN-13-2740

Medium (DMEM; Thermo Fisher Scientific) supplemented with 10% FBS (Thermo Fisher Scientific), 1% Glutamine (Thermo Fisher Scientific), and 1% penicillin/streptomycin (Thermo Fisher Scientific). MCF7-GFP and LNCaP-GFP cancer cells, established in our laboratory, were cultured in DMEM and RPMI (*Hyclone*), respectively, supplemented with 10% FBS, 1% Glutamine, and 1% penicillin/streptomycin.

L-NNA (N_ω-nitro-L-arginine), an irreversible inhibitor of NOS1 and a reversible inhibitor of NOS2; PTIO (2-phenyl-4,4,5,5-tetramethylimidazoline-1-oxyl 3-oxide), a NO-scavenger; the NO-donor SNAP (S-nitroso-N-acetyl-D L-penicillamine); BSO (L-buthionine-sulfoximine), a glutathione-synthesis inhibitor; H_2O_2, DMNQ (2,3-dimethoxy-1,4-naphthoquinone), a stimulator of superoxide production, and crystal violet were purchased from Sigma-Aldrich. Recombinant CXCL14 was purchased from R&D Systems and Peprotech with no difference in performance in our hands.

The antibodies detecting NOS1 (Cell Signaling Technology), *Nitrotyrosine*, N-tyr, *clone 1A6* (Millipore), pERK and ERK (Cell Signaling Technology), and α-tubulin (Sigma-Aldrich) as loading control were used for Western blot analyses. Primary antibodies recognizing CD31 (BD Biosciences), F4/80 (AbD Serotec), CD68 (AbD Serotech), LYVE-1 (Reliatech), and panNOS (Abcam), in addition to peroxidase-coupled secondary antibodies, were used to stain human and mouse tissue by immunohistochemistry and immunofluorescence.

Establishment of fibroblast derivatives with stable knockdown of NOS1

Fibroblast derivatives with stable knockdown of *Nos1* were established as described in Supplementary Materials and Methods.

Immunohistochemistry, quantitative real-time PCR, immunoblotting analysis

Immunohistochemistry, immunofluorescence, immunoblotting, and quantitative real-time PCR (qRT-PCR) analyses were performed as previously described (8). Immunohistochemistry staining was quantified by grading the fraction of stained area of each tumor section on a scale ranging from 0 (no signal) to 5 (signals distributed over the whole section). Immunoblotting signals were monitored by ImageQuant LAS4000 (GE Healthcare) and quantified using Image J (http://imagej.nih.gov/ij). The qRT-PCR primer (Sigma-Aldrich) used to study gene expression is listed in Supplementary Materials and Methods.

Transfection of siRNA

Fibroblasts (2.5×10^3) were seeded per well of a 96-well plate. The next day 100 nmol/L siRNA, target-specific and nontargeting control, was transfected into fibroblasts using Polyfect reagent (Qiagen). The cells were incubated for 24 hours in presence of the transfection mixture and then medium was replaced by serum-reduced DMEM. The number of cells after growth for 3 days under low serum conditions was determined by crystal violet staining (see Supplementary Material and Methods).

To analyze the efficiency of siRNA-mediated knockdown, 8×10^4 fibroblasts were seeded per well of a 6-well plate. The cells were transfected with target-specific or nontargeting siRNA using Polyfect. Medium was changed to serum-reduced DMEM the next day and cells were lysed to extract RNA according to the manufacturer's protocol (GenElute; Sigma-Aldrich).

Cell-based assays

The different assays used to analyze cell growth and migration, reactive oxygen species (ROS) and glutathione levels, and the activation of the antioxidant response element (ARE)- and HIF1α response element (HRE) are described in detail in Supplementary Materials and Methods.

Xenograft study

Animal experiments were conducted in accordance with national guidelines and approved by the Stockholm North Ethical Committee on Animal Experiments, and performed similar to as previously described (8). In brief, 2×10^6 cancer cells (LNCaP or MCF7) admixed with 1.2×10^5 fibroblasts (NIH-ctr/shCtr, NIH-CXCL14/shCtr, NIH-CXCL14/shN1:1, and NIH-CXCL14/shN1:3) were injected s.c. in the right flank of 5- to 7-week-old severe combined immunodeficient (SCID) mice. Tumor growth was followed over time by palpating the tumors twice per week. When tumors reached a size between 600 and 900 mm^3, mice were sacrificed and tumors were frozen in liquid nitrogen and stored at −75°C for subsequent immunohistochemical and qRT-PCR analyses.

Statistical analyses

All data are expressed as the mean SEM. GraphPad Prism 5.0d for Mac (GraphPad Software) was used for all statistical analyses. Student unpaired two-tailed *t* tests, Mann–Whitney, one-way ANOVA with Newman–Keuls Multiple Comparison post-tests and two-way ANOVA with Bonferroni post-tests were performed to determine if differences among different experimental groups or treatment conditions are statistically significant. Spearman correlation was used to analyze a potential correlation between two different experimental parameters (*, $P < 0.05$; **, $P < 0.01$).

Results

NOS1 expression is enhanced in CXCL14 fibroblasts

To further understand the enhanced protumoral effects of CXCL14-expressing fibroblasts, as compared with control fibroblast, a comparative gene expression analysis was performed. This analysis demonstrated that more than 600 genes showed a larger than 2.5-fold differential expression (unpublished observation).

Among the upregulated genes, *Nos1* was selected for further analyses. NOS1, nitric oxide synthase 1 or nNOS, is one of three isoforms of nitric oxide synthases (NOS). NOS1, NOS2 (iNOS), and NOS3 (eNOS), and their product nitric oxide (NO) exert profound effects on both malignant and nonmalignant cells and tissues (10). Thus, NOS1 seemed as a potential candidate that functionally contributes to the different effects associated with the protumorigenic action of CXCL14-expressing fibroblasts (8).

Upregulation of NOS1 mRNA and protein in cultured CXCL14 fibroblasts was confirmed by qRT-PCR, immunoblotting, and immunocytochemistry (Fig. 1A and B). In contrast, *Nos3* was not upregulated in CXCL14 fibroblasts, and *Nos2* was not expressed by NIH fibroblasts (Fig. 1A). Increased expression of NOS1 was also demonstrated in LNCaP/NIH-CXCL14 tumors by immunohistochemical analysis of tumor sections (Fig. 1C). NOS1 was detected mainly in the nucleus of cultured fibroblasts (Fig. 1B) and in fibroblasts of xenograft tumors (Fig. 1C). Tumor expression of *Nos1* correlated significantly with *CXCL14* levels ($r = 0.797$; $P = 0.0029$) in LNCaP/NIH-ctr and LNCaP/NIH-CXCL14 tumors, suggesting a functional link between those two factors (Fig. 1D). Furthermore, stimulation of NIH-ctr fibroblasts with recombinant CXCL14 induced expression of *Nos1* over time (Supplementary Fig. S1A), thus establishing a connection between CXCL14-induced signaling and *Nos1* expression.

Analysis of human prostate tumor material, using a panNOS antibody, also demonstrated NOS expression in prostate cancer, including focal expression in tumor stroma (Fig. 1E).

Upregulation of NOS1 is associated with increased protein nitration, but not with increased NO secretion

The upregulation of NOS1 suggests a concomitant increased production and release of NO by CXCL14 fibroblasts. However, NIH-CXCL14 cells did not secrete enhanced levels of NO into the surrounding medium compared with NIH-ctr (Fig. 2A). Moreover, introduction of the NO-donor SNAP demonstrated that the SNAP-stimulated NO release is quenched in NIH-CXCL14 compared with control fibroblasts (Fig. 2A). These data indicate that NOS1-derived NO is rather consumed in intracellular processes. The finding that CXCL14 fibroblasts displayed a higher degree of tyrosine nitration compared with control fibroblasts (Fig. 2B) supports this idea. Tyrosine nitration is an irreversible posttranslational modification of increasingly recognized importance and indicative of nitrosative stress caused by elevated NO levels (11).

To gain further insight in the role of NOS1 in CXCL14 fibroblasts, derivatives with stable knockdown of *Nos1* (designated shN1:1, shN1:2, shN1:3) were established. Successful knockdown of NOS1 in NIH-CXCL14 cells was confirmed on protein (Fig. 2B) and mRNA level (Supplementary Fig. S2). Tyrosine nitration in NIH-CXCL14 cells was reduced in the *Nos1*-knockdown derivatives in a manner that paralleled the level of *Nos1* knockdown (Fig. 2B). Finally, enhanced activation of the mitogen-activated protein kinase pathway in CXCL14 fibroblasts, as compared with control fibroblasts, was also affected by impaired NOS1 expression, suggesting that NOS1/NO is implicated in the induction of this signaling pathway (Fig. 2B).

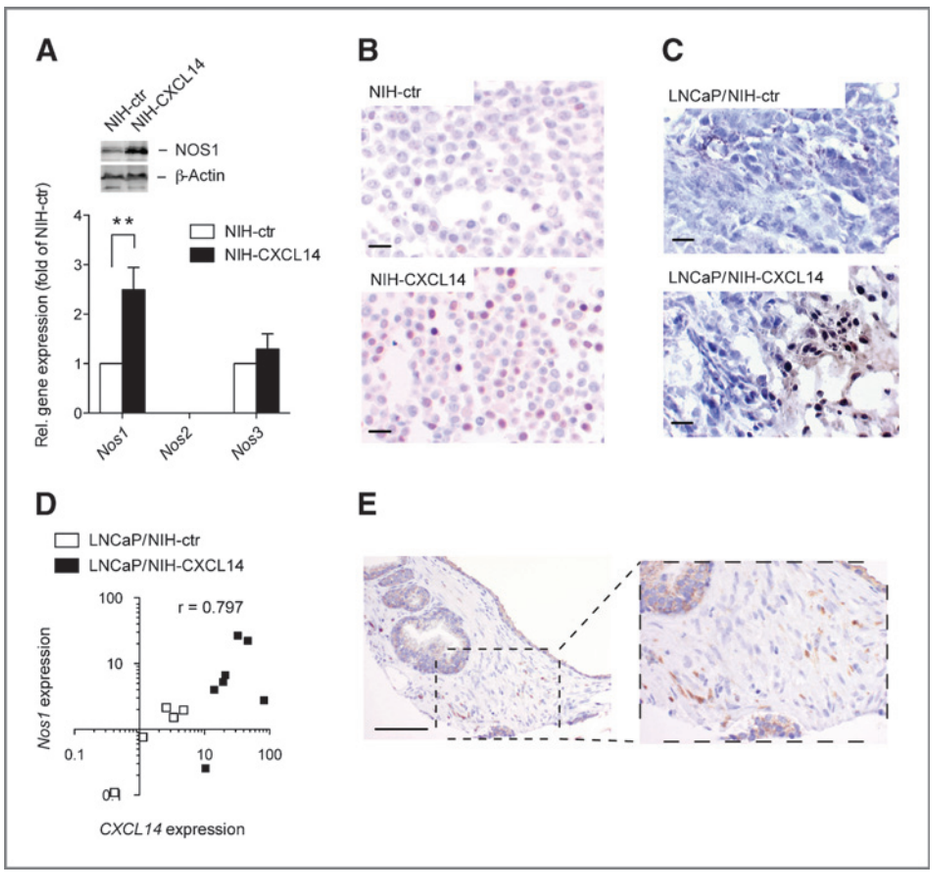

Figure 1. Enhanced expression of NOS1 in CXCL14 fibroblasts. A, detection of *Nos1*, *Nos2*, and *Nos3* expression in NIH-ctr (□) and NIH-CXCL14 (■) fibroblasts by immunoblotting (top) and qRT-PCR (bottom). Data, mean ± SEM. **, $P < 0.01$ (two-way ANOVA). B and C, NOS1 immunostaining of paraffin-embedded NIH-ctr and NIH- CXCL14 fibroblasts (B), and LNCaP prostate xenograft tumors (C). Scale bars, 20 μm. D, comparison of *CXCL14* and *Nos1* mRNA levels in the LNCaP/fibroblast tumor xenograft. r, the Spearman correlation coefficient. E, NOS expression in human prostate cancer specimen detected by immunohistochemistry using a panNOS antibody. Scale bar, 100 μm. Data in A are derived from five independent experiments. Data in D are based on the analyses of five and seven LNCaP/NIH-ctr and LNCaP/NIH-CXCL14 tumor xenografts, respectively.

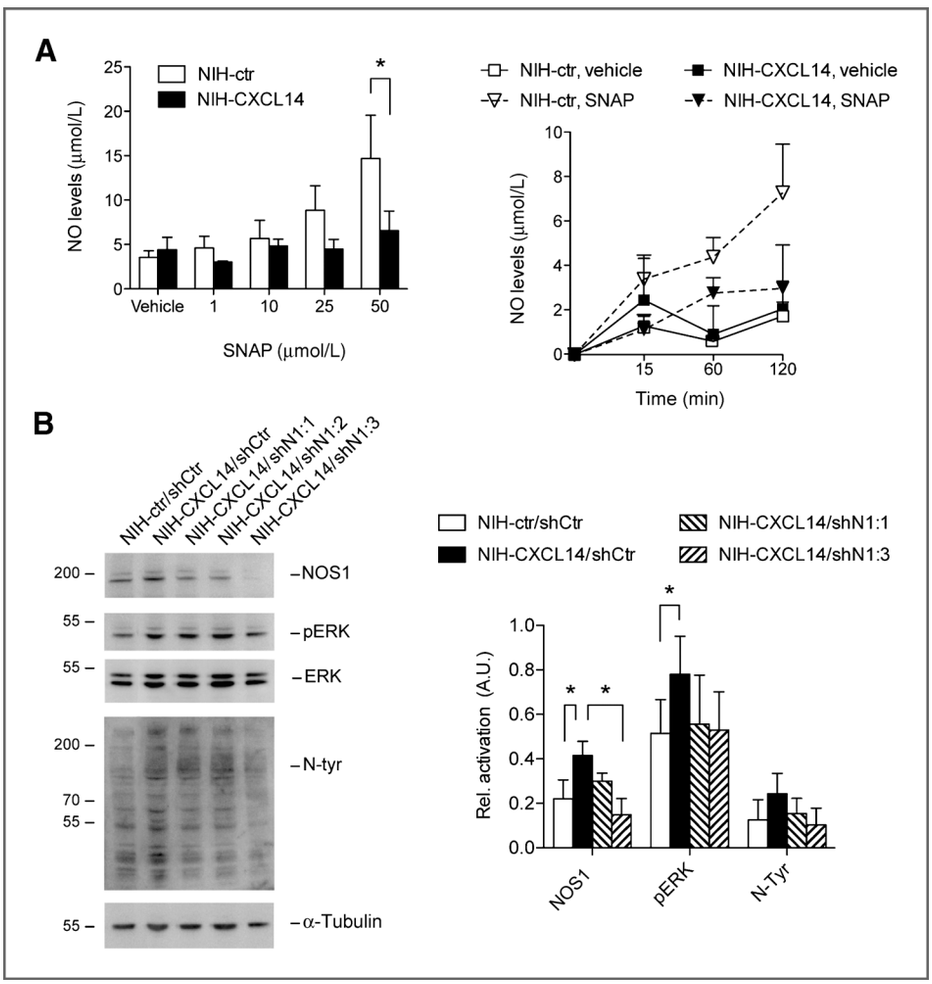

Figure 2. Upregulation of NOS1 is associated with increased protein nitration, but not with increased NO secretion. A, NO secretion into conditioned medium by NIH-ctr and NIH-CXCL14 fibroblasts cultured in serum-reduced medium was measured in the absence or presence of different concentrations of the NO-donor SNAP for 15 minutes (left) and at different time points after stimulation with vehicle or 10 μmol/L SNAP (right). Data, mean ± SEM. *, $P < 0.05$ (two-way ANOVA). B, NOS1 expression, ERK activation, and tyrosine nitration were measured by immunoblotting in cell lysates of the NIH-ctr and NIH-CXCL14 derivatives stably expressing either nontargeting shRNA (shCtr) or different *Nos1*-targeting shRNA (shN1:1, shN1:2, shN1:3) as indicated (see Material and Methods for details). Data in A are derived from four independent experiments. Data in B shows the quantification of three independent immunoblot analyses as the mean ± SEM. *, $P < 0.05$ (one-way ANOVA).

These data support the view that the increased NO, derived from enhanced NOS1 expression in CXCL14 fibroblasts, is used in intracellular processes, rather than being secreted.

Induction of NOS1 expression is a consequence of oxidative stress in CXCL14 fibroblasts

Signaling by NO is closely linked to the action of ROS and *vice versa* (11). Because CXCL14 induced the formation of ROS in fibroblasts (Fig. 3A), and the CXCL14-stimulated induction of *Nos1* occurred after the induction of heme oxygenase 1 (*Hmox1* or *HO-1*), an indicator of oxidative stress (Supplementary Fig. S1A), we entertained the possibility that upregulation of NOS1 in NIH-CXCL14 cells is a consequence of ROS-induced oxidative stress in these fibroblasts.

Evidence of increased oxidative stress in NIH-CXCL14 cells was provided by analyses using an ARE-coupled reporter that monitors the activity of NRF2, a transcription factor activated upon oxidative stress that controls a transcriptional program regulating cellular stress signaling (12, 13). Treatment of NIH-ctr cells with DMNQ, a compound stimulating superoxide production in cells, clearly stimulated the ARE promotor (Fig. 3B). Comparison of NIH-ctr and NIH-CXCL14 cells revealed a similarly pronounced activation of the ARE reporter in CXCL14 fibroblasts (Fig. 3B). Furthermore, the expression level of the NRF2-target *Hmox1* was clearly enhanced in NIH-CXCL14 cells (Supplementary Fig. S1B). In line with recent findings suggesting a link between NO, NRF2, and activation of HIF1α signaling (14, 15), an enhanced activation of the HIF1α response element HRE in NIH-CXCL14 cells was also detected (Supplementary Fig. S3). Interestingly, short-term stimulation of fibroblasts with CXCL14 failed to induce a robust NRF2 and HIF1α response, suggesting that the increased ARE and HRE activity observed in CXCL14 fibroblasts represents an adaptation of fibroblasts to a chronic stimulation with CXCL14 (Fig. 3B). Increased oxidative stress in NIH-CXCL14 cells, compared with NIH-ctr cells, was also indicated by increased levels of total and oxidized glutathione (Fig. 3C).

Next, we investigated if NOS1 expression could be induced as a result of oxidative stress in fibroblasts. DMNQ-derived superoxide significantly stimulated the expression of NOS1 in NIH-ctr cells, in an antioxidant sensitive manner (Fig. 3D and Supplementary Fig. S4). Furthermore, DMNQ also promoted tyrosine nitration, and this effect was even more pronounced in the presence of N-acetyl-L-cysteine (NAC; Fig. 3D), compatible

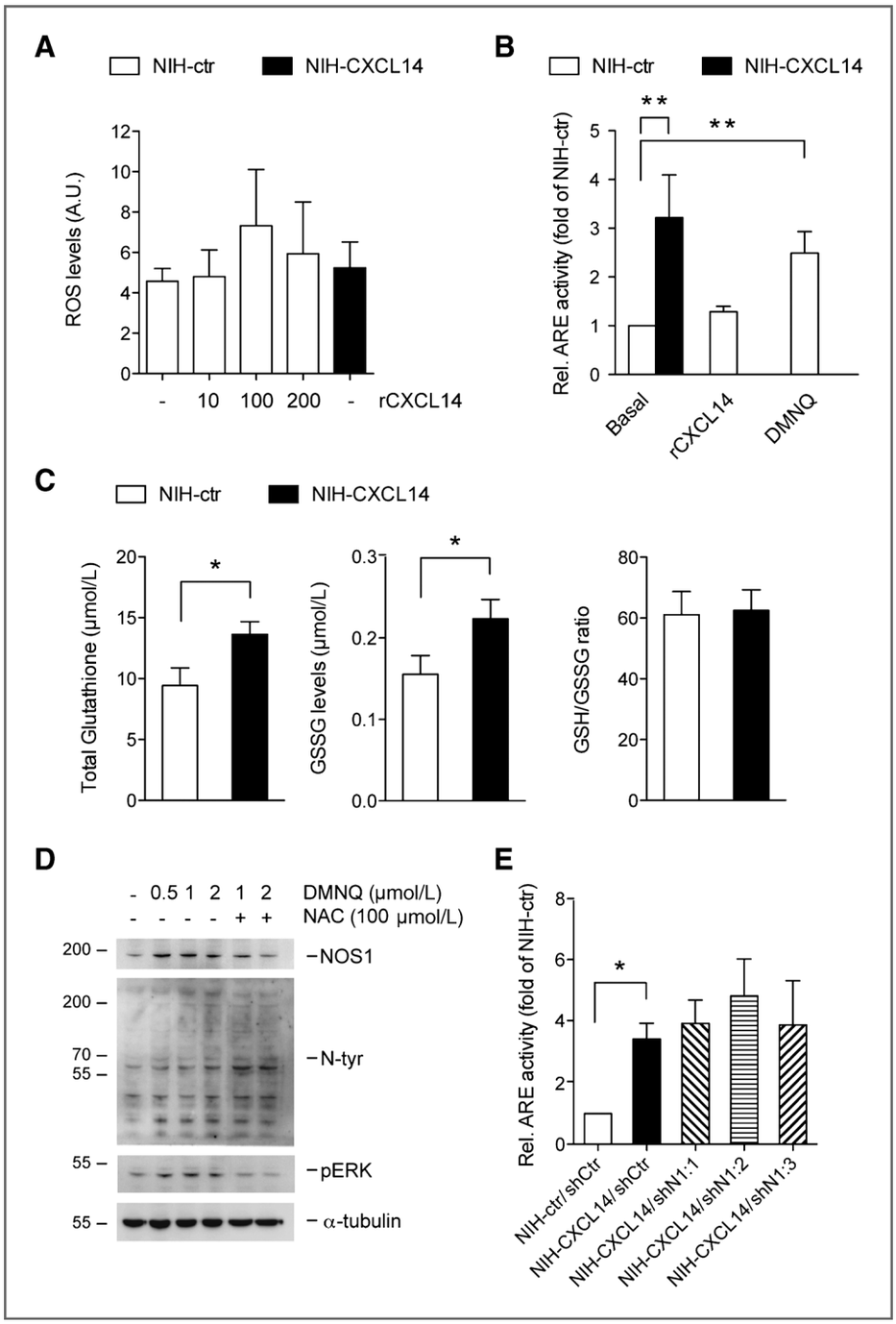

Figure 3. CXCL14 fibroblasts display characteristics of oxidative stress. A, ROS measurements using H_2DFFDA in NIH-ctr (□) and NIH-CXCL14 (■) cells under basal culture conditions, and after stimulation of NIH-ctr with different concentrations of recombinant CXCL14 (rCXCL14) in serum-reduced medium. Data, mean ± SEM. B, reporter gene-assay comparing the induction of the ARE reporter in NIH-ctr (□) and NIH-CXCL14 (■) cells, and in NIH-ctr cells stimulated with 200 ng/mL CXCL14 or 2 µmol/L DMNQ. Data, mean ± SEM. **, $P < 0.01$ (one-way ANOVA). C, comparison of glutathione (GSH; left) and oxidized glutathione (GSSG; middle) levels and GSSG/GSH ratio (right) of NIH-ctr (□) and NIH-CXCL14 (■) cells growing under serum-reduced culture conditions. Data, mean ± SEM. *, $P < 0.05$ (*t* test). D, NOS1 expression, ERK activation, and tyrosine nitration in unstimulated and DMNQ-treated NIH-ctr cells, with or without NAC, were measured by immunoblotting analyses of total cell lysates. E, reporter gene-assay comparing the induction of the ARE reporter in NIH-ctr and NIH-CXCL14 derivatives stably expressing either nontargeting shRNA (shCtr) or different *Nos1*-targeting shRNA (shN1:1, shN1:2, shN1:3) as indicated. Data, mean ± SEM. *, $P < 0.05$ (one-way ANOVA). Data in A, B, C, and E are derived from four to six independent analyses. Data in D show representative results from three independent analyses.

with previous data demonstrating a role of ROS in restricting NO signaling (16). Moreover, the enhanced ARE signaling in CXCL14 fibroblasts was not compromised by *Nos1* downregulation (Fig. 3E), supporting the hypothesis that the increased production of ROS occurs upstream of NOS1 induction.

These data raised the possibility that NOS1-derived NO is used to balance increased ROS levels in CXCL14 fibroblasts. Accordingly, sequestration of NO in NIH-CXCL14 cells would increase intracellular ROS levels and, thus, strengthen the dependence of these cells on other ROS scavenging systems such as glutathione. To test this hypothesis, the growth of NIH-CXCL14 cells was analyzed in presence of the NO scavenger PTIO or BSO, an inhibitor of glutathione synthesis, or when using both compounds in combination (Supplementary Fig. S5A). CXCL14 fibroblasts were particularly sensitive to the combined treatment of BSO and PTIO. The growth-inhibitory effect of the combination was about 56% compared with 35% (BSO) and 17% (PTIO) of the single agents and indicative of cell

death, in contrast with the mono-treatment (Supplementary Fig. S5A). A similar effect was observed in BSO-treated CXCL14 fibroblasts with suppressed NOS1 expression (Supplementary Fig. S5B). This implies that the BSO-mediated increase in ROS levels is cytotoxic in the absence of NO, and confirms the ROS-balancing effect of NOS1-derived NO.

Together, these findings demonstrate that oxidative stress promotes NOS1 expression in fibroblasts, and more specifically suggest that oxidative stress contributes to the induction of NOS1 in CXCL14 fibroblasts.

NOS1 contributes to the growth and migration of CXCL14 fibroblasts

CXCL14 fibroblasts have previously been shown to exhibit functional properties of CAFs (8). However, mRNA levels of fibronectin (*Fn1*), collagen (*Col1a1, Col18a*), and α smooth muscle actin (αSMA; *Acta2*), the proto-typical marker of myofibroblasts, were not elevated in NIH-CXCL14 compared with NIH-ctr cells (Supplementary Fig. S6A). Furthermore, NIH-CXCL14 cells did not show an enhanced ability to contract collagen (Supplementary Fig. S6B). Despite the lack of abundant *Acta2* expression, CXCL14 fibroblasts expressed enhanced levels of other CAF markers, such as decorin (*Dcn*), vimentin (*Vim*), *Fgf2*, and *Fsp1/ S100A4* (Supplementary Fig. S6A). Fsp1 has been proposed as a marker of a functionally discrete CAF subtype (17). The expression level of tenascin C (*Tnc*), previously shown to be associated with the Fsp1-positive CAF subtype (18), was also enhanced in NIH-CXCL14 compared with NIH-ctr cells. In contrast, expression of *Pdgfra* and *Pdgfrb*, both marker of additional CAF subsets, was not induced in NIH-CXCL14 fibroblasts (Supplementary Fig. S6A). Importantly, NOS1 was found to affect the expression of some of these factors such as *Fsp1, Vim, Fn1*, and *Fgf2* (Supplementary Fig. S6A).

To evaluate the importance of increased NOS1 levels on functional properties of CXCL14 fibroblasts, we studied the *in vitro* behavior of NIH-CXCL14 cells under various conditions of impaired NOS1/NO signaling. Using cell counting and proliferation assays, we have previously demonstrated that NIH-CXCL14 cells are able to proliferate under low serum conditions (1% FBS), whereas NIH-ctr fibroblasts are not (8). These earlier findings were confirmed using a crystal violet-based assay (Fig. 4). Experiments with the NOS inhibitor L-NNA (Fig. 4A) and PTIO (Fig. 4B) demonstrated that both agents significantly reduced the growth rate of NIH-CXCL14 cells without major effects on the growth of control fibroblasts.

To more directly investigate the importance of NOS1 for the growth of NIH-CXCL14 cells under low serum conditions, experiments with *Nos1*-targeting siRNA were performed. Impaired *Nos1* expression reduced NIH-CXCL14 fibroblast growth as compared with cells transfected with control siRNA (Fig. 4C). This NOS1-dependent growth of NIH-CXCL14 cells was also confirmed when cell growth was determined by cell counting (Fig. 4D).

Although NOS1 is important for the stimulation of CXCL14-fibroblast growth, it seemed to be dispensable for the growth of these cells under conditions of oxidative stress (Supplementary Fig. S7A). Interestingly, NOS1 was found to act as an important mediator of the NIH-CXCL14–supported growth of prostate and breast cancer cells exposed to an oxidizing environment (Supplementary Fig. S7B).

Upregulation of CXCL14 in fibroblasts is also associated with increased migration of these cells (8). This behavior is—at least in part—dependent on the NOS1/NO axis, as the migration of NIH-CXCL14 cells was reduced by PTIO (Fig. 4E).

Together, these experiments demonstrate that the upregulation of NOS1 in CXCL14 fibroblasts is functionally linked to the migratory and proliferative *in vitro* phenotypes of these cells.

NOS1 depletion in CXCL14 fibroblasts reduces their tumor-supportive capacity *in vivo*

To assess the importance of NOS1/NO in the protumorigenic effects of CXCL14-expressing fibroblasts, we compared NIH-ctr/shCtr, NIH-CXCL14/shCtr, and two different NIH-CXCL14 derivatives with diminished *Nos1* expression (shN1:1 and shN1:3), in the LNCaP coinjection tumor model. As shown in Fig. 5A, downregulation of *Nos1* in the CXCL14-overexpressing fibroblasts significantly reduced tumor growth in this prostate cancer model.

The effects of fibroblast-derived CXCL14, and its potential NOS1 dependency, were also investigated in a breast cancer model in which three different fibroblasts (NIH-ctr/shCtr, NIH-CXCL14/shCtr, NIH-CXCL14/shN1:3) were coinjected with the estrogen receptor–positive breast cancer cells MCF7. These experiments demonstrated, even more clearly than the prostate cancer model, an enhanced tumor-supportive ability of CXCL14 fibroblasts (NIH-CXCL14/shCtr) and a critical role of NOS1 in the CXCL14 fibroblasts in this process (Fig. 5A).

It was noted in both the breast and prostate cancer model that the diminished tumor growth mediated by *Nos1* knockdown in CXCL14 fibroblasts was not fully reduced to the level of the control (NIH-ctr/ shCtr) tumors (Fig. 5A). This suggests that also other NOS1-independent mechanisms contribute to the tumor-promoting effect of CXCL14 fibroblasts.

A specific comparison of the early growth of tumors demonstrated that NIH-CXCL14/shCtr fibroblasts seemed to be particularly efficient in supporting the initial growth (0–15 mm^3) of the prostate and breast tumors (Fig. 5B). This effect was reduced in developing tumors with CXCL14 fibroblasts lacking NOS1 expression (shN1:1 and shN3), implying a critical role of NOS1 in tumor initiation.

These experiments thereby demonstrate that enhanced NOS1 expression is causally linked to the tumor-supportive capacity of CXCL14 fibroblasts and particularly involved in the early phase of tumor development.

NOS1 downregulation reduces tumor macrophage infiltration in CXCL14 tumors

LNCaP/NIH-CXCL14 tumors are characterized by increased vessel density and increased macrophage infiltration, as compared with LNCaP/NIH-ctr tumors (8). Analyses of CD31 immunostaining of tumor sections confirmed the previous observation of increased vessel density in LNCaP/NIH-CXCL14/shCtr tumors compared with LNCaP/NIH-ctr/shCtr tumors (Supplementary Fig. S8A). This difference also remained when the number of vessels was analyzed separately.

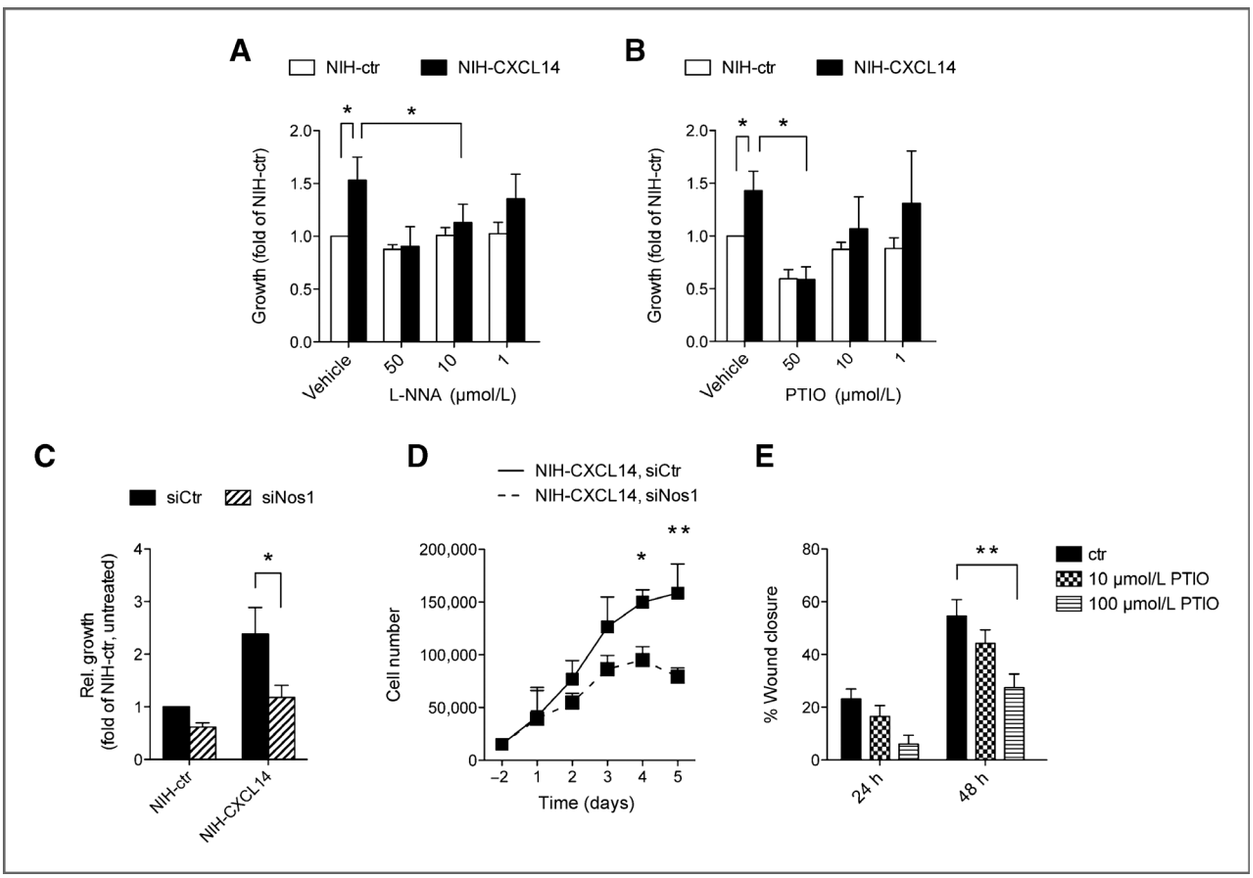

Figure 4. Diminished growth and migration of CXCL14 fibroblasts under NOS/NO inhibition. NIH-ctr (□) and NIH-CXCL14 (■) cells were cultured for 3 days in serum-reduced medium alone or serum-reduced medium supplemented with HCl (vehicle), the NOS inhibitor L-NNA (A) or the NO scavenger PTIO (B). The growth of fibroblasts, NIH-ctr and NIH-CXCL14, was studied after transfection of nontargeting siRNA (siCtr) or *Nos1*-specific siRNA. After transfection of the cells, medium was changed to serum-reduced condition and cultures were maintained for 3 days (C) or for the indicated number of days (D). Data, mean ± SEM. *, $P < 0.05$; **, $P < 0.01$ (two-way ANOVA). Growth was determined by measuring the absorbance of crystal violet-stained fixed cells (A–C) and cell counting (D). E, migration of CXCL14 fibroblasts was analyzed in a wound healing assay after culture of cells in the presence of vehicle (HCl) or different concentrations of the NO scavenger PTIO. The width of the wound of crystal violet-stained cells was determined after 24 and 48 hours of culture in serum-reduced medium. Data, mean ± SEM. **, $P < 0.01$ (two-way ANOVA). Data in A–E are derived from four to six independent analyses, each performed in quadruplicates.

However, downregulation of *Nos1* in CXCL14 fibroblasts did not have a major impact on vessel number and density (Supplementary Fig. S8A). No CXCL14- and/or NOS1-dependent effects on vessel density were observed in the experimental breast tumors (Supplementary Fig. S8B). We noted that the proportion of blood vessels was in general much higher in the breast compared with the prostate cancer model, suggesting tumor-type–dependent differences and breast tumors being less sensitive to the proangiogenic effect of CXCL14 fibroblasts. Additional analyses revealed that fibroblast-derived CXCL14 promoted the ingrowth of lymphatic vessels in both LNCaP and MCF7 tumors. However, this effect was not dependent on the presence of fibroblast-expressed NOS1 (Supplementary Fig. S9B).

In agreement with previous findings (8), the number of infiltrating macrophages was increased in LNCaP/NIH-CXCL14/shCtr tumors (Fig. 6A). Importantly, a reduction in macrophages was observed in the LNCaP tumors following downregulation of *Nos1* in the NIH-CXCL14 cells (Fig. 6A). The same pattern—but even more prominent—was observed in the breast cancer model. The clearly increased infiltration of macrophages in MCF/NIH-CXCL14:shCtr tumors was significantly diminished in tumors with *Nos1* knockdown in the CXCL14 fibroblasts (Fig. 6B).

Together, these data implicate NOS1 as an important determinant of the protumorigenic effects of CXCL14 fibroblasts in the prostate and breast cancer model, and also suggest regulation of macrophage infiltration as one contributing mechanism.

Discussion

The present study identifies NOS1 as a novel, oxidative stress-induced integral component of CXCL14 signaling in fibroblasts (Figures 1–3), which contributes to the autocrine promigratory and proproliferative effects of CXCL14 (Figure. 4). Besides CXCL14, ROS and NO have been shown to be

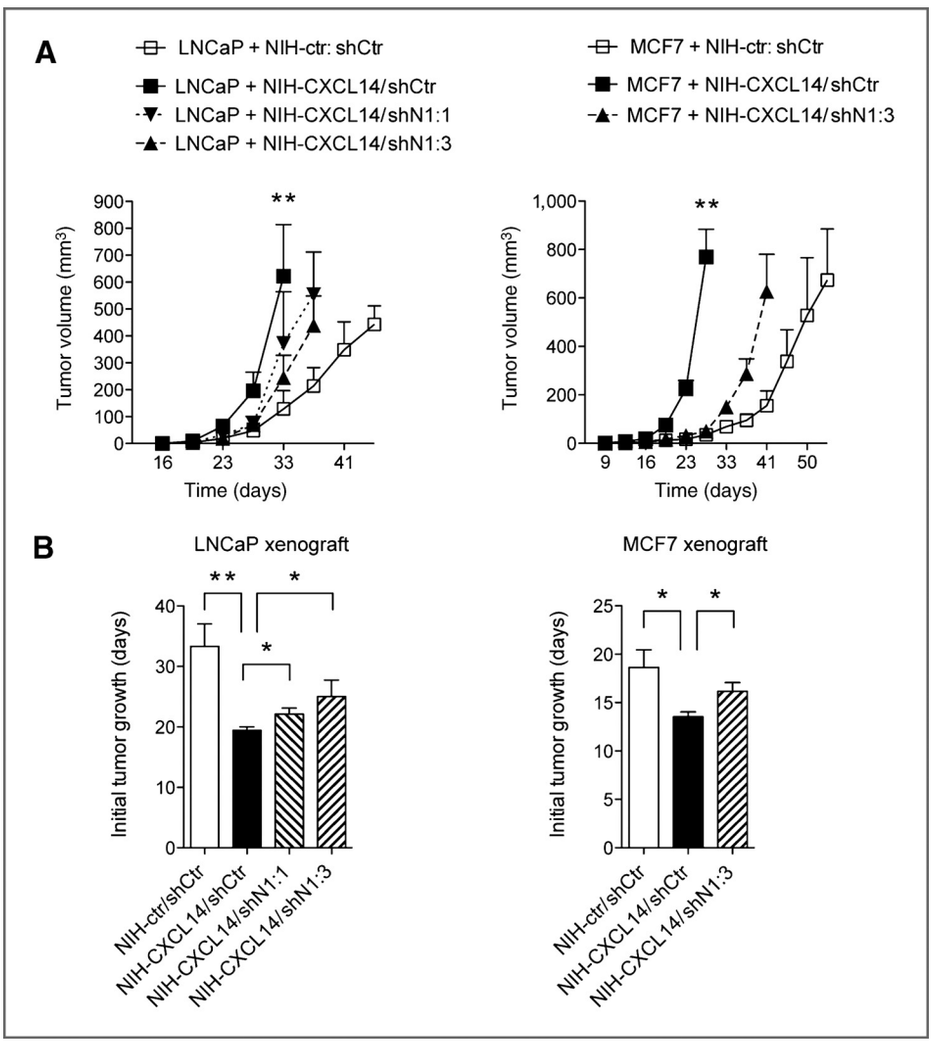

Figure 5. NOS1 is a mediator of the protumorigenic effect of CXCL14 fibroblasts. A, growth curves of tumors derived from coinjection of LNCaP (left) and MCF7 (right) cancer cells together with the fibroblasts indicated s.c. into SCID mice. Data, mean ± SEM. **, $P < 0.01$ (two-way ANOVA). B, length of time to reach 15 mm^3 tumor size of indicated LNCaP (left) and MCF7 (right) tumor xenografts. Data, mean ± SEM. *, $P < 0.05$; **, $P < 0.01$ (one-way ANOVA). Data in A and B are derived from tumor groups composed of $n = 5$ to 7 animals per group.

associated with CCL5 and CXCL12 signaling (19–21), proposing ROS and NO as general mediators of chemokine signaling. Importantly, CXCL14-induced NOS1 also plays a crucial role in the ability of CXCL14 fibroblasts to promote tumor growth *in vivo* (Fig. 5), including tumor macrophage recruitment (Fig. 6). The clinical relevance of the connection between *Nos1* and *CXCL14* revealed in experimental settings (Fig. 1D) was substantiated by significant associations of these factors in two different collections of clinical tumor samples (Supplementary Fig. S10; refs. 22, 23). This study thus identifies NOS1/NO signaling as a potential target for interference with the functions of protumoral CXCL14 fibroblasts.

The increased expression of NOS1 in CXCL14 fibroblasts was not accompanied by enhanced secretion of NO from these cells (Fig. 2A). We therefore conclude that the NOS1-derived increased NO is predominantly used in chemical reactions controlling intracellular processes. This is supported by evidence of NOS1-dependent enhanced tyrosine nitration found in CXCL14 fibroblasts (Fig. 2B). Tyrosine nitration occurs as a result of elevated NO levels causing nitrosative stress (11), and has recently been recognized as an important posttranslational modification for chemokines with strong impact on their mode of action (24). In addition, intracellular NO in NIH-CXCL14 cells may be converted to different reactive nitrogen species (RNS), signaling molecules with a broad range of effects from stimulating proliferation to cell killing (25, 26). A significant proportion of NOS1 was detected in the nucleus of cultured fibroblasts, and nuclear NOS1 was also observed in prostate xenograft tumors (Figure 1B and C). Nuclear NOS1 has previously been linked to transcriptional regulation, as for example shown by its effect on the action of the SP1 transcription factor (27). Also, a recent study focusing on NOS3 described nuclear complexes composed of NOS3/HIF1α and NOS3/ERβ in prostate cancer cells (28). Together, these findings suggest that NOS1-dependent phenotypes of NIH-CXCL14 fibroblasts are largely independent of secreted NO, and rather occur as a result of intracellular effects of NO, eventually supplemented by NOS1-regulated transcriptional changes.

Enhanced oxidative stress was uncovered as another characteristic of CXCL14 fibroblasts as demonstrated through findings of increased activity of the NRF2-controlled ARE reporter (Fig. 3B) and increased levels of total and oxidized

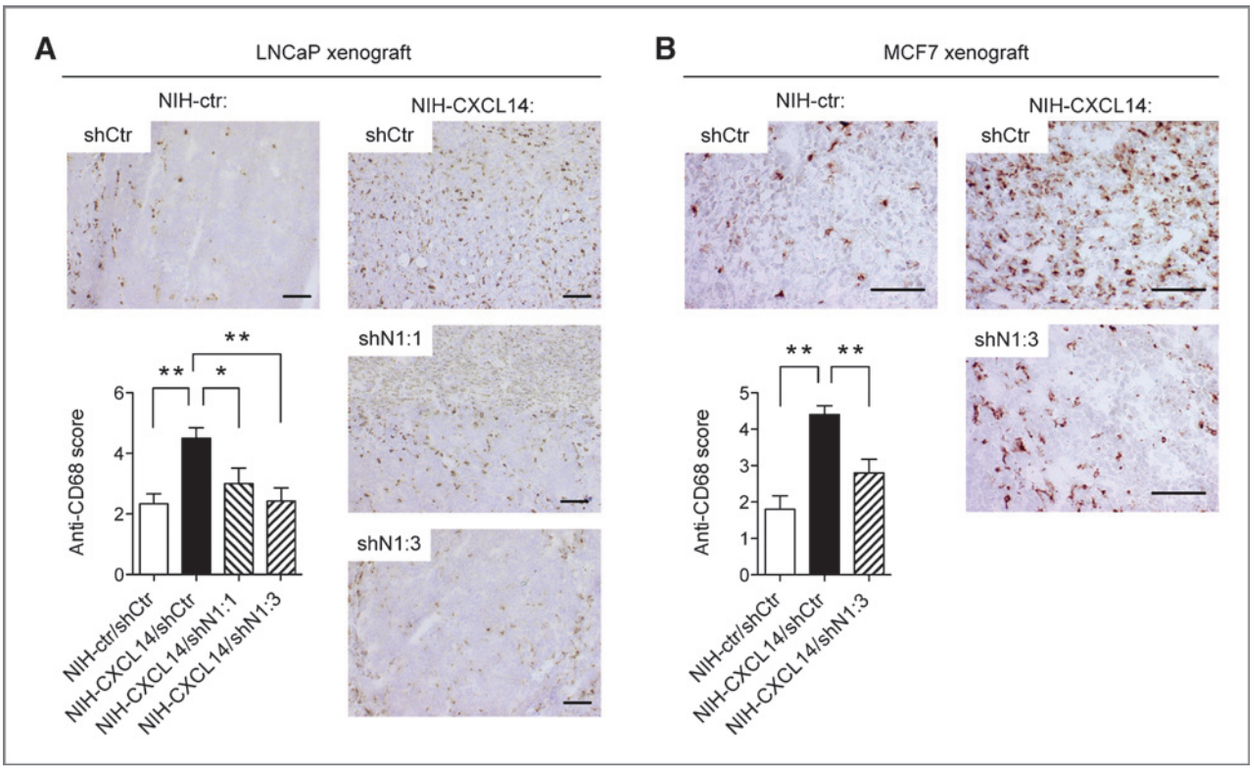

Figure 6. NOS1 downregulation reduces tumor macrophage infiltration in NIH-CXCL14 tumors. Representative micro-photographs (left) and quantifications (right) of macrophage content in LNCaP (A) and MCF7 (B) tumor xenografts determined by CD68 immunohistochemistry of LNCaP and MCF7 tumors, respectively. A scoring system ranging from 0 to 5 (no staining to abundant staining) was applied to evaluate the immunohistochemistry signals in the core of the tumor. Quantifications are derived from analyses of seven tumors of each of the experimental groups. Data in A and B, mean ± SEM. **, $P < 0.01$ (one-way ANOVA). Scale bars in A and B, 100 μm.

glutathione (Fig. 3C). Both occurred in the absence of an apparent increase in steady-state levels of ROS (Fig. 3A). The oxidative stress response is concluded to seem upstream of NOS1 induction, since ARE activity was not affected by NOS1 downregulation in NIH-CXCL14 cells (Fig. 3E). This notion is further supported by the observation that the induction of *Hmox1*, a factor expressed upon oxidative stress, preceded Nos1 induction in CXCL14-stimulated fibroblasts (Supplementary Fig. S1). Moreover, NOS1 expression was triggered by oxidative stress in fibroblasts (Fig. 3D). A similar redox-phenotype, characterized by an adaptive response to ROS, including an activated NRF2 pathway and increased glutathione levels, but absence of increased ROS levels, was recently described also in fibroblasts endogenously expressing oncogenic RAS (29). Interestingly, HIF1α signaling, evident by stimulation of a HRE reporter, was also augmented in CXCL14 fibroblasts (Supplementary Fig. S2). To what extent this response is responsible for the previously described upregulation of angiogenic factors in CXCL14 fibroblasts (8) should be investigated in future studies. The increased nuclear expression of NOS1 and activation of HIF1α signaling in NIH-CXCL14 cells (Fig. 1 and Supplementary Fig. S2) suggests a similar regulation as previously described for NOS3 that forms complexes with HIF1α, HIF2α, and other transcription factors in the nucleus of prostate cancer cells (28). Importantly, this study also demonstrated that increased nuclear expression of NOS3 and HIF2α is associated with bad prognosis in prostate cancer, suggesting clinical relevance of this signaling.

The presence of oxidative stress, and the increased expression of NOS1 in CXCL14 fibroblasts suggested a connection between enhanced ROS and NOS1/NO signaling. The relevance of the reciprocal, multilayered interplay of ROS and NO is well established. ROS, on the one hand, have been shown to constrain NO-induced signaling (16). In return, NO can act as a powerful antioxidant (30), and reactions of ROS and NO can give rise to various RNS (11). We conclude from the ROS-induced NOS1 expression (Fig. 3D) and the NOS1-independent, increased activation status of the HIF1α and NRF2 pathway in NIH-CXCL14 derivatives (Fig. 3E) that upregulation of NOS1 occurs in response to CXCL14-induced oxidative stress. Furthermore, NOS1-derived NO seems to control, in concert with other upregulated ROS scavengers (e.g., glutathione), the extent of ROS formation and oxidative stress levels in CXCL14 fibroblasts. It is well established that the local production and intracellular flux of ROS needs to be tightly regulated. A physiologic increase of intracellular ROS can stimulate, e.g., cell proliferation, whereas high ROS levels can have detrimental effects, eventually leading to cell death (31). An ROS-induced NOS expression has been described in other cell types, including prostate cancer cells and endothelial cells (32, 33).

Upregulation of NOS and NO thus seems as a common and integrated part of an adaptive response to oxidative stress. Finally, downregulation of *Nos1*, or NO scavenging with PTIO, renders NIH-CXCL14 cells particularly sensitive to BSO-mediated glutathione depletion, thus suggesting a functional interplay between the glutathione and NOS1 system in the oxidative stress response of NIH-CXCL14 cells (Supplementary Fig. S3A and S3B).

Beside a role in ROS detoxification, the concomitant induction of NOS1 and ROS scavengers also enhances the capacity of CXCL14 fibroblasts to handle increased amounts of ROS, NO, and/or RNS that would otherwise have an adverse effect. Interestingly, we found that NIH-CXCL14 cells promote the initial growth of LNCaP and MCF7 tumors *in vivo* in which tumors pass a hypoxic phase, and this ability was clearly impaired in CXCL14-fibroblast derivatives with *Nos1* knockdown (Fig. 5B). This implies a NOS1/NO-dependent production of paracrine-acting factors by CXCL14 fibroblasts that support the growth of cancer cells in an oxidative stress-inducing microenvironment. This notion is further supported by the evidence for an involvement of NOS1 in the paracrine effects of CXCL14 fibroblasts under conditions of oxidative stress (Supplementary Fig. S7B). The identification of these paracrine factors and inhibition of their action is an important task for future studies that might present novel strategies to block early tumor growth. Other recent studies have also recognized the importance of ROS- and NOS/NO-induced signaling pathways in the establishment of a myofibroblast/CAF-phenotype with tumor-promoting activity (34, 35).

The present study provides evidence that enhanced NOS1 expression in NIH-CXCL14 cells contributes to their previously described CAF-phenotype that is characterized by cell autonomous and paracrine protumoral effects. *Nos1* downregulation, or treatment with NO scavengers, neutralized the increased *in vitro* migration and proliferation of NIH-CXCL14 cells (Fig. 4). The analyses of the protumorigenic effects of CXCL14 fibroblasts in this study extend the findings of our previous study by showing enhanced protumoral effects of CXCL14 fibroblast also in a MCF7 model of breast cancer (Fig. 5). About the mechanisms that are involved in this effect, the present study identifies enhanced lymphangiogenesis as a novel phenotype induced by CXCL14 fibroblasts in LNCaP and MCF7 tumors (Supplementary Fig. S5), besides the increased blood vessel infiltration previously described in the prostate cancer model (8). Importantly, the tumor-promoting effect of CXCL14 fibroblasts was clearly diminished when the expression of NOS1 is impaired in these fibroblasts (Fig. 5). It is noted that this occurs in the absence of a major impact on blood and lymphatic vessels recruitment. This implicates other, NOS1/NO-independent pathways, in the regulation of these processes, such as signaling induced by HIF1α, the prototypic stimulator of angiogenesis whose activity is enhanced in NIH-CXCL14 cells and not affected by *Nos1* knockdown (Supplementary Fig. S2). Another putative candidate mediator is HMOX1, which was found to be upregulated in NIH-CXCL14 cells (Supplementary Fig. S1B) and induced upon CXCL14 stimulation of fibroblasts (Supplementary Fig. S1A). HMOX1 is an enzyme with multimodal effects and has previously been shown to mediate cellular effects of the chemokine CXCL12 (36). Moreover, HMOX1 can stimulate angiogenesis and is involved in the recruitment and activation of inflammatory cells into tumors (37).

In contrast with the vascular effects, enhanced macrophage infiltration in CXCL14 tumors in both tumor models was significantly reduced following downregulation of NOS1 in the CXCL14 fibroblasts (Fig. 6). These findings strongly suggest the recruitment of macrophages as one particularly NOS1-dependent effect of the CXCL14 fibroblasts. The protumorigenic effects of macrophages are well described and linked to their polarization adopting the M2 phenotype (38, 39). It will be an important topic for further studies to characterize the interplay between CXCL14, CXCL14-producing fibroblasts, macrophage recruitment, polarization, and tumor growth in more detail. In light of the recent finding that tyrosine nitration changes the chemoattractant spectrum of the chemokine CCL2 (24), and that NOS1 is important for macrophage accumulation in CXCL14 tumors, it will be interesting to address if tyrosine nitration is also important for CXCL14-mediated macrophage recruitment and the adoption of a protumorigenic phenotype, for example by modification of CXCL14 itself or other monocyte-attracting chemokines induced in CXCL14 fibroblasts.

Interestingly, analysis of different CAF markers revealed upregulation of *Fsp1* but not *Acta2*, *Pdgfra*, and *Pdgfrb* in NIH-CXCL14 cells compared with NIH-ctr fibroblasts (Supplementary Fig. S6). Recently, Cortez and colleagues divided the heterogeneous population of CAFs in four discrete, marker-based CAF subsets characterized by either αSMA (*Acta2*), FSP1, PDGFR-α, or PDGFR-β expression, respectively. (17). FSP1-expressing CAFs (CAF^{FSP1}) are characterized by VEGFA and Tenascin C expression, and have been shown to promote the recruitment of macrophages into the tumor (18, 40). These are also features of the CXCL14-expressing fibroblasts (Fig. 6 and Supplementary Fig. S6), providing evidence for the idea that CXCL14 fibroblasts belong to CAF^{FSP1} subset. Of note, both the enhanced expression of FSP1 by CXCL14 fibroblasts and their stimulation of macrophage recruitment are partially mediated by NOS1 (Fig. 6 and Supplementary Fig. S6), underlining the importance of NOS1 in determining the CAF-phenotype of CXCL14 fibroblasts.

In summary, this study identifies NOS1, NRF2, and HIF1α signaling as previously unrecognized components of autocrine CXCL14 signaling. The NOS1 effects seem largely independent of paracrine NO effects, because NO secretion is not increased in CXCL14 fibroblasts. The data clearly demonstrate that NOS1-induced signals are of major importance for the protumoral effects of CXCL14-expressing fibroblasts and thus suggest novel therapeutic possibilities. Finally, the findings of the study should also encourage continued studies on the role of NOS1 in the intracellular signaling of other chemokines.

Disclosure of Potential Conflicts of Interest

No potential conflicts of interest were disclosed.

Authors' Contributions

Conception and design: M. Augsten, A. Östman

Development of methodology: M. Augsten
Acquisition of data (provided animals, acquired and managed patients, provided facilities, etc.): M. Augsten, E. Sjöberg, S.U. Vorrink, Å. Borg, A. Östman
Analysis and interpretation of data (e.g., statistical analysis, biostatistics, computational analysis): M. Augsten, E. Sjöberg, O. Frings, S.U. Vorrink, J. Frijhoff, E. Olsson, A. Östman
Writing, review, and/or revision of the manuscript: M. Augsten, Å. Borg, A. Östman
Administrative, technical, or material support (i.e., reporting or organizing data, constructing databases): J. Frijhoff
Study supervision: A. Östman

Acknowledgments

The authors thank Anna-Karin Persson and the staff of the animal facility at Department of Microbiology, Tumor and Cell Biology, Karolinska Institutet, for their continuous support with the animal experiments, Jörn Hanusch for providing the LNCaP-GFP derivatives, and Sandra Luecke at Department of Cell and Molecular Biology, Karolinska Institutet, for kindly sharing HRE and ARE reporter constructs.

Grant Support

A. Östman received grants from the Swedish Cancer Society, and a Linné-grant to STARGET from the Swedish Research Council.

The costs of publication of this article were defrayed in part by the payment of page charges. This article must therefore be hereby marked *advertisement* in accordance with 18 U.S.C. Section 1734 solely to indicate this fact.

Received September 23, 2013; revised February 20, 2014; accepted March 7, 2014; published OnlineFirst April 7, 2014.

References

1. Hara T, Tanegashima K. Pleiotropic functions of the CXC-type chemokine CXCL14 in mammals. J Biochem 2012;151:469–76.
2. Meuter S, Schaerli P, Roos RS, Brandau O, Bosl MR, von Andrian UH, et al. Murine CXCL14 is dispensable for dendritic cell function and localization within peripheral tissues. Mol Cell Biol 2007;27:983–92.
3. Gu XL, Ou ZL, Lin FJ, Yang XL, Luo JM, Shen ZZ, et al. Expression of CXCL14 and its anticancer role in breast cancer. Breast Cancer Res Treat 2012;135:725–35.
4. Ozawa S, Kato Y, Kubota E, Hata R. BRAK/CXCL14 expression in oral carcinoma cells completely suppresses tumor cell xenografts in SCID mouse. Biomed Res 2009;30:315–8.
5. Shellenberger TD, Wang M, Gujrati M, Jayakumar A, Strieter RM, Burdick MD, et al. BRAK/CXCL14 is a potent inhibitor of angiogenesis and a chemotactic factor for immature dendritic cells. Cancer Res 2004;64:8262–70.
6. Shurin GV, Ferris RL, Tourkova IL, Perez L, Lokshin A, Balkir L, et al. Loss of new chemokine CXCL14 in tumor tissue is associated with low infiltration by dendritic cells (DC), while restoration of human CXCL14 expression in tumor cells causes attraction of DC both in vitro and in vivo. J Immunol 2005;174:5490–8.
7. Allinen M, Beroukhim R, Cai L, Brennan C, Lahti-Domenici J, Huang H, et al. Molecular characterization of the tumor microenvironment in breast cancer. Cancer Cell 2004;6:17–32.
8. Augsten M, Hagglof C, Olsson E, Stolz C, Tsagozis P, Levchenko T, et al. CXCL14 is an autocrine growth factor for fibroblasts and acts as a multi-modal stimulator of prostate tumor growth. Proc Natl Acad Sci U S A 2009;106:3414–9.
9. Kurth I, Willimann K, Schaerli P, Hunziker T, Clark-Lewis I, Moser B. Monocyte selectivity and tissue localization suggests a role for breast and kidney-expressed chemokine (BRAK) in macrophage development. J Exp Med 2001;194:855–61.
10. Fukumura D, Kashiwagi S, Jain RK. The role of nitric oxide in tumour progression. Nat Rev Cancer 2006;6:521–34.
11. Thomas DD, Ridnour LA, Isenberg JS, Flores-Santana W, Switzer CH, Donzelli S, et al. The chemical biology of nitric oxide: implications in cellular signaling. Free Radic Biol Med 2008;45:18–31.
12. Osburn WO, Kensler TW. Nrf2 signaling: an adaptive response pathway for protection against environmental toxic insults. Mutat Res 2008;659:31–9.
13. Sporn MB, Liby KT. NRF2 and cancer: the good, the bad and the importance of context. Nat Rev Cancer 2012;12:564–71.
14. Berchner-Pfannschmidt U, Tug S, Kirsch M, Fandrey J. Oxygen-sensing under the influence of nitric oxide. Cell Signal 2010;22:349–56.
15. Kim TH, Hur EG, Kang SJ, Kim JA, Thapa D, Lee YM, et al. NRF2 blockade suppresses colon tumor angiogenesis by inhibiting hypoxia-induced activation of HIF-1alpha. Cancer Res 2011;71:2260–75.
16. Thomas DD, Ridnour LA, Espey MG, Donzelli S, Ambs S, Hussain SP, et al. Superoxide fluxes limit nitric oxide-induced signaling. J Biol Chem 2006;281:25984–93.
17. Cortez E, Roswall P, Pietras K. Functional subsets of mesenchymal cell types in the tumor microenvironment. Semin Cancer Biol 2014;25:3–9.
18. O'Connell JT, Sugimoto H, Cooke VG, MacDonald BA, Mehta AI, LeBleu VS, et al. VEGF-A and Tenascin-C produced by S100A4+ stromal cells are important for metastatic colonization. Proc Natl Acad Sci U S A 2011;108:16002–7.
19. Hiasa K, Ishibashi M, Ohtani K, Inoue S, Zhao Q, Kitamoto S, et al. Gene transfer of stromal cell-derived factor-1alpha enhances ischemic vasculogenesis and angiogenesis via vascular endothelial growth factor/endothelial nitric oxide synthase-related pathway: next-generation chemokine therapy for therapeutic neovascularization. Circulation 2004;109:2454–61.
20. Qiu L, Ding L, Huang J, Wang D, Zhang J, Guo B. Induction of copper/zinc-superoxide dismutase by CCL5/CCR5 activation causes tumour necrosis factor-alpha and reactive oxygen species production in macrophages. Immunology 2009;128:e325–34.
21. Zheng H, Dai T, Zhou B, Zhu J, Huang H, Wang M, et al. SDF-1alpha/CXCR4 decreases endothelial progenitor cells apoptosis under serum deprivation by PI3K/Akt/eNOS pathway. Atherosclerosis 2008;201:36–42.
22. Finak G, Bertos N, Pepin F, Sadekova S, Souleimanova M, Zhao H, et al. Stromal gene expression predicts clinical outcome in breast cancer. Nat Med 2008;14:518–27.
23. Muggerud AA, Hallett M, Johnsen H, Kleivi K, Zhou W, Tahmasebpoor S, et al. Molecular diversity in ductal carcinoma in situ (DCIS) and early invasive breast cancer. Mol Oncol 2010;4:357–68.
24. Molon B, Ugel S, Del Pozzo F, Soldani C, Zilio S, Avella D, et al. Chemokine nitration prevents intratumoral infiltration of antigen-specific T cells. J Exp Med 2011;208:1949–62.
25. Nathan C. Specificity of a third kind: reactive oxygen and nitrogen intermediates in cell signaling. J Clin Invest 2003;111:769–78.
26. Szabo C, Ischiropoulos H, Radi R. Peroxynitrite: biochemistry, pathophysiology and development of therapeutics. Nat Rev Drug Discov 2007;6:662–80.
27. Baldelli S, Aquilano K, Rotilio G, Ciriolo MR. Glutathione and copper, zinc superoxide dismutase are modulated by overexpression of neuronal nitric oxide synthase. Int J Biochem Cell Biol 2008;40:2660–70.
28. Nanni S, Benvenuti V, Grasselli A, Priolo C, Aiello A, Mattiussi S, et al. Endothelial NOS, estrogen receptor beta, and HIFs cooperate in the activation of a prognostic transcriptional pattern in aggressive human prostate cancer. J Clin Invest 2009;119:1093–108.
29. DeNicola GM, Karreth FA, Humpton TJ, Gopinathan A, Wei C, Frese K, et al. Oncogene-induced Nrf2 transcription promotes ROS detoxification and tumorigenesis. Nature 2011;475:106–9.
30. Wink DA, Miranda KM, Espey MG, Pluta RM, Hewett SJ, Colton C, et al. Mechanisms of the antioxidant effects of nitric oxide. Antioxid Redox Signal 2001;3:203–13.
31. Stone JR, Yang S. Hydrogen peroxide: a signaling messenger. Antioxid Redox Signal 2006;8:243–70.
32. Wartenberg M, Schallenberg M, Hescheler J, Sauer H. Reactive oxygen species-mediated regulation of eNOS and iNOS expression in multicellular prostate tumor spheroids. Int J Cancer 2003;104:274–82.

33. Zhen J, Lu H, Wang XQ, Vaziri ND, Zhou XJ. Upregulation of endothelial and inducible nitric oxide synthase expression by reactive oxygen species. Am J Hypertens 2008;21:28–34.
34. Martinez-Outschoorn UE, Balliet RM, Rivadeneira DB, Chiavarina B, Pavlides S, Wang C, et al. Oxidative stress in cancer associated fibroblasts drives tumor-stroma co-evolution: a new paradigm for understanding tumor metabolism, the field effect and genomic instability in cancer cells. Cell Cycle 2010;9:3256–76.
35. Toullec A, Gerald D, Despouy G, Bourachot B, Cardon M, Lefort S, et al. Oxidative stress promotes myofibroblast differentiation and tumour spreading. EMBO Mol Med 2010;2:211–30.
36. Deshane J, Chen S, Caballero S, Grochot-Przeczek A, Was H, Li Calzi S, et al. Stromal cell-derived factor 1 promotes angiogenesis via a heme oxygenase 1-dependent mechanism. J Exp Med 2007;204:605–18.
37. Was H, Dulak J, Jozkowicz A. Heme oxygenase-1 in tumor biology and therapy. Curr Drug Targets 2010;11:1551–70.
38. Condeelis J, Pollard JW. Macrophages: obligate partners for tumor cell migration, invasion, and metastasis. Cell 2006;124:263–6.
39. Mantovani A, Sozzani S, Locati M, Allavena P, Sica A. Macrophage polarization: tumor-associated macrophages as a paradigm for polarized M2 mononuclear phagocytes. Trends Immunol 2002;23:549–55.
40. Zhang J, Chen L, Xiao M, Wang C, Qin Z. FSP1+ fibroblasts promote skin carcinogenesis by maintaining MCP-1-mediated macrophage infiltration and chronic inflammation. Am J Pathol 2011;178:382–90.